SCIENCE AND TECHNOLOGY ORGANIZATION
CENTRE FOR MARITIME RESEARCH AND EXPERIMENTATION

Reprint Series **CMRE-PR-2019-062**

AUV active perception: Exploiting the water column

Andrea Munafó, Gabriele Ferri, Kevin LePage, Ryan Goldhahn

June 2019

Originally published in:

OCEANS 2017 - Aberdeen, UK, 19-22 June 2017,
doi: 10.1109/OCEANSE.2017.8084874

About CMRE

The Centre for Maritime Research and Experimentation (CMRE) is a world-class NATO scientific research and experimentation facility located in La Spezia, Italy.

The CMRE was established by the North Atlantic Council on 1 July 2012 as part of the NATO Science & Technology Organization. The CMRE and its predecessors have served NATO for over 50 years as the SACLANT Anti-Submarine Warfare Centre, SACLANT Undersea Research Centre, NATO Undersea Research Centre (NURC) and now as part of the Science & Technology Organization.

CMRE conducts state-of-the-art scientific research and experimentation ranging from concept development to prototype demonstration in an operational environment and has produced leaders in ocean science, modelling and simulation, acoustics and other disciplines, as well as producing critical results and understanding that have been built into the operational concepts of NATO and the nations.

CMRE conducts hands-on scientific and engineering research for the direct benefit of its NATO Customers. It operates two research vessels that enable science and technology solutions to be explored and exploited at sea. The largest of these vessels, the NRV Alliance, is a global class vessel that is acoustically extremely quiet.

CMRE is a leading example of enabling nations to work more effectively and efficiently together by prioritizing national needs, focusing on research and technology challenges, both in and out of the maritime environment, through the collective Power of its world-class scientists, engineers, and specialized laboratories in collaboration with the many partners in and out of the scientific domain.

NOTE: The CMRE Reprint series reprints papers and articles published by CMRE authors in the open literature as an effort to widely disseminate CMRE products. Users are encouraged to cite the original article where possible.

AUV Active Perception: Exploiting the Water Column

Andrea Munafò *†, Gabriele Ferri†, Kevin LePage†, Ryan Goldhahn‡,
*Marine Autonomous and Robotic Systems
National Oceanography Centre, European Way, Southampton, UK, SO14 3ZH
Email: andmun@noc.ac.uk
†NATO STO Centre for Maritime Research and Experimentation, La Spezia, Italy
Email: {gabriele.ferri, kevin.lepage}@cmre.nato.int
‡Lawrence Livermore National Laboratory, Livermore, CA
Email: goldhahn1@llnl.gov

***Abstract*—Autonomous Underwater Vehicles (AUVs) present a low-cost alternative or supplement to existing underwater surveillance networks. The NATO STO Centre for Maritime Research and Experimentation is developing collaborative autonomous behaviours to improve the performance of multi-static networks of AUVs. In this work we lay the foundation to combine a range-dependent acoustic model with a three dimensional measurement model for a linear array within a Bayesian framework. The resulting algorithm is able to provide the vehicles with an estimation of the target depth together with the more usual information based on a planar assumption (i.e. target latitude and longitude). Results are shown through simulations and as obtained from the REP16 sea trial where for the first time a preliminary implementation of the method was deployed in the C-OEX vehicles.**

I. Introduction

The usual approach in ocean exploration, surveillance and reconnaissance is based on using active or passive sonar systems composed of either source-receiver pairs (active sonars), or receivers only (passive sonars) [1]. When arrays of sensors are available as receivers [2], they can be used to perform spatial filtering of the signals incident upon it [3], thereby providing directionality information (i.e. the ability to discriminate from which direction the signal is being radiated). Traditionally, these systems are deployed on vessels, frigates or submarines which, being equipped with towed arrays, represent the assets of surveillance networks. However, this approach is platform and manpower intensive, hence very costly. Autonomous Underwater Vehicles (AUVs) have recently gained a great interest in many applications in underwater surveillance due to their low cost, covertness, persistencyy, together with their ability to being equipped with high performance sensors. In [4] an experimental network composed of mobile and fixed nodes was deployed off the coast of Norway with the objective of creating an integrated security system which could include aerial, terrestrial and underwater assets for the protection of off-shore and coastal installations. The usage of AUVs for ASW has been proposed in [5] where rather than performing ASW with a single, large, highly capable, capital ship or submarine, the authors propose to have a system of many, small, limited capability, low-cost systems working in concert. The sensors and underwater assets make collaborative decisions independent of an operator and carry out the necessary changes to their actions. A more recent approach has been described in [6] where the vehicle autonomy is linked together with the on-board real-time tracker so that the vehicle can optimally modify its trajectory to be in the best position to lock on the potential target, hence minimising the expected target position error and increasing its ability to maintain tracks. As opposed to more traditional assets, these small, comparatively low-cost and low-power vehicles are characterised by very limited computational and communication capabilities [7], [8], [9]. However, when these robots are deployed in large numbers and properly interconnected [10], [11], they can create an intelligent network that is able to go beyond the limitations of the individual sensors, to achieve a network gain, with important features of scalability, robustness, and reliability. One attempt to move into this direction was reported in [12] where the authors resolve the port-starboard ambiguity coming from the usage of linear arrays sharing information between the nodes of the network, hence exploiting the spatial diversity that is obtained using different sensors at once. Similar concepts are also discussed in [13] where the AUVs/nodes of a multi-static sensor network share local information, namely contacts and tracks, demonstrating that the system increases its robustness and resilience. This paper extends previous work in several important ways. We borrow from [13] the idea of using a range-dependent acoustic model to calculate the predicted probability of target detection P_D. This P_D is then combined within a Bayesian framework to compute a posterior distribution for the target location at each ping. This approach has been generalised and a three dimensional measurement model has been devised to optimally solve the problem of 3D localisation of an underwater target. Using this information, the vehicles can then collectively decide their position in the 3D environment to optimise some mission-driven measurements of the network performance. The resulting approach overcomes the known right-left or port-starboard ambiguity created by the cylindrical symmetry of a single line of hydrophones [14] proposing a unified framework in which the ambiguity is instead utilised for the robot advantages. This fits inside the concept of "active perception", which requires robots that can both estimate quantities of interest and autonomously take actions to improve those estimates [15]. The promising effectiveness of the method is shown through simulations and at-sea results as obtained during the recent Recognized Environmental Picture (REP) Atlantic 2016 sea trial where one AUV was deployed and successfully reduced its uncertainty in

determining the depth of an echo-repeat target.

The rest of the document is organised as follows: The extension from a planar bistatic localisation to a three dimensional scenario is presented in Section II. How to use this information as a measurement model is described in Section III, and its integration within a particle filter that is able to provide the vehicles with a full posterior on the target state is described in Section III-B. Computer simulations to show the effectiveness of the approach are reported in Section IV, and results from a recent sea-trial in Section V. Finally, conclusions are drawn in Section VI.

II. 3D BISTATIC LOCALISATION

The typical approach to quantify bistatic contact localisation relies on a planar assumption where the contributions of varying source, target and receiver depths on the distances and angles are neglected [16]. This is usually justified by the typical geometries of interest in many surveillance applications, where the target can be considered far from the sonar elements (i.e. source and receivers). The planar assumption simplifies the problem and allows to have simple equations to calculate the estimated target position given the measured quantities: the propagation time τ and the bearing θ, relative to the array heading ϕ^R, as produced by the array signal processing [14].

In usual AUV set-ups, receiving sensors are composed of uniformly spaced linear arrays, with a beamformed output that is cylindrically symmetric. In the planar case, this means that it is not possible to discriminate if an echo is detected from the port or starbord side of the array (port-starboard or left-right ambiguity).

It is not possible to rely on the planar assumption when the target is close to the source or the receiver of the sonar, in this case in fact the depth component has a non negligible impact that needs to be accounted for. Furthermore, the left-right ambiguity generated in the case of the planar assumption is usually seen as a complication with an impact on the detection and tracking capability, leading often to performance degradation [12].

When the problem is tackled as a three dimensional scenario, although the geometry becomes more complicated, interesting new features emerge, such as the possibility of tracking the depth of the target, and to include the port-starboard ambiguity into a unified formulation.

The measured quantities are the same as per the planar case. More in details, we consider:

- τ is the measured propagation time from source to receiver
- θ is the measured bearing from receiver to target, and relative to the array bearing
- ϕ^R is the array heading
- ψ^R is the array pitch
- receiver location: $\mathbf{x}^R = [x^R, y^R]^\top$
- source location: $\mathbf{x}^S = [x^S, y^S]^\top$
- average speed of sound c

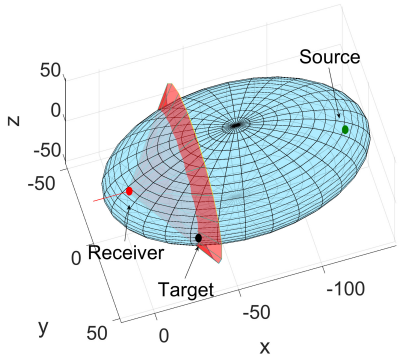

Fig. 1. Bistatic source-target-receiver geometry in the three dimensional case. The target lies on the intersection between the bistatic ellipsoid and the beamforming ambiguity cone of the linear array.

Fig. 1 illustrates the source-target-receiver geometry in the bistatic case. The target estimated position can be obtained intersecting the bistatic ellipsoid (obtained once the measured propagation time from source to receiver is available) with the cone of ambiguity coming out of the linear array beamforming (i.e. the cone that is obtained once θ, the measured bearing from receiver to target, and relative to the array bearing is available).

Defining, R_ψ as the rotation matrix around the y-axis (pitch), and R_ϕ as the rotation matrix around the z-axis (heading), the bistatic ellipsoid with center in $\mathbf{x}_c = (\mathbf{x}^S + \mathbf{x}^R)/2$, can be defined, in the inertial frame $< I >$, as:

$$(\mathbf{x} - \mathbf{x}_c) * R^\top_{\psi_e,\phi_e} * A * R_{\psi_e,\phi_e} * (\mathbf{x} - \mathbf{x}_c) = 1 \qquad (1)$$

where:

$$A = \begin{bmatrix} 1/a^2 & 0 & 0 \\ 0 & 1/b^2 & 0 \\ 0 & 0 & 1/d^2 \end{bmatrix} \qquad (2)$$

with $a = c\tau/2$, $b^2 = a^2 - C^2$, and $C = ||\mathbf{x}^S - \mathbf{x}^R||$, and $d = b$.

$$R_{\psi_e,\phi_e} = R_{\psi_e} R_{\phi_e}, \qquad (3)$$

$$\phi_e = -tan^{-1}\left(\frac{y^S - y^R}{x^S - x^R}\right), \qquad (4)$$

$$\psi_e = \frac{\pi}{2} - acos\left(\frac{z^S - z^R}{||\mathbf{x}^S - \mathbf{x}^R||}\right). \qquad (5)$$

The ellipsoid (1) can be expressed into the receiver's body frame $< b >$, i.e. the reference frame centered at the location of the receiver $\mathbf{x}^R$ and with the x-axis aligned to the surge direction, applying

$$\mathbf{x}_b = R^\top_{\psi,\phi}\mathbf{x} - R^\top_{\psi,\phi}\mathbf{x}^R \qquad (6)$$

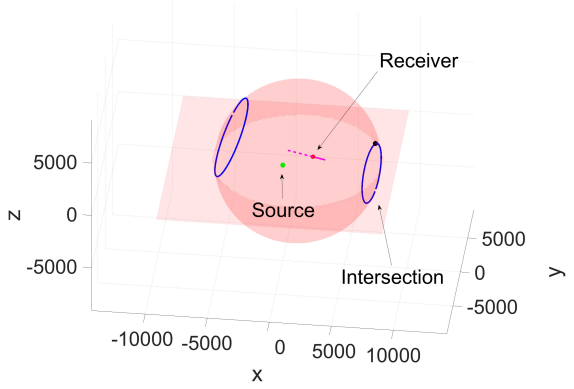

Fig. 2. Linear array ambiguity as obtained from 10. The source is located in $\mathbf{x}^S = (0, 0, 0)$, the receiver at $\mathbf{x}^R = (2250, 1500, 0)$ with a pitch $\psi^R = 20\,\text{deg}$ and heading $\phi^R = 10\,\text{deg}$. The target is shown as a black filled circle.

where ψ^R is the array pitch angle, and ϕ^R is the array heading.

In the receiver's body frame, the array ambiguity cone (i.e. a cone with aperture along the x-axis of the body frame) can be expressed, in cylindrical coordinates r, Ψ as:

$$x_b = r/R, \tag{7}$$
$$y_b = rcos(\Psi), \tag{8}$$
$$z_b = rsin(\Psi). \tag{9}$$

where $R = tan(\theta)$ determines the aperture of the cone and it depends on the measured bearing θ, and $\Psi = [0, 2\pi]$.

The intersection (in the vehicle's body frame) between the bistatic ellipse and the array ambiguity cone is finally obtained substituting (9) into (6), as a function of the cylindrical coordinates r, Ψ:

$$A(\Psi)_b r^2 + B(\Psi)_b r + C(\Psi)_b = 0; \tag{10}$$

where $A(\Psi)_b$, $B(\Psi)_b$ and $C(\Psi)_b$ are the coefficients of the equations and depend on the specific source-receiver-target geometry.

It is usually more convenient to express equation (10) in Cartesian coordinates in the inertial frame. This can be done applying (9) and the inverse of (6): $\mathbf{x} = R_{\psi,\phi}\mathbf{x}_b + \mathbf{x}^R$

Fig. 2 shows an example of intersection between the bistatic ellipse and the ambiguity cone of the linear array. Note that applying (10) two intersecting curves are obtained, one per each of the nappes of the double cone. Disambiguation between the two can easily be done using the array measured bearing θ.

III. Localisation of a target

A. Measurement model

We consider the case where the team's only way of sensing the target is through a uniform linear array able to measure, at time t, the signal bistatic propagation time τ_t from source to target to receiver, and the bearing θ_t from the receiver to the target.

Let $\mathbf{x}^S(t) = \left[x_t^S, y_t^S, z_t^S\right]^\top$ be the source position at time t, while the receiver position at t is $\mathbf{x}^R(t) = \left[x_t^S, y_t^S, z_t^S\right]$ and its heading and pitch are $\mathbf{p}^R(t) = \left[\phi_t^R, \psi_t^R\right]$.

Given the array produced measurements, the associated measurement function is:

$$\mathbf{z(t)} = \begin{bmatrix}\tau_t \\ \theta_t\end{bmatrix} \tag{11}$$

where

$$\begin{bmatrix}\tau_t \\ \theta_t\end{bmatrix} = \begin{bmatrix}||\mathbf{x}^T(t) - \mathbf{x}^R(t)|| + ||\mathbf{x}^T(t) - \mathbf{x}^S(t)|| + w^\tau(t) \\ -acos\left(\frac{\langle \mathbf{x}^T(t) - \mathbf{x}^R(t), \mathbf{v}^R(t)\rangle}{||\mathbf{x}^T(t) - \mathbf{x}^R(t)||||\mathbf{v}^R(t)||}\right) + w^\theta(t)\end{bmatrix}$$

$$\mathbf{w(t)} = \begin{bmatrix}w^\tau(t) \\ w^\theta(t)\end{bmatrix} \sim \mathcal{N}\left(\begin{bmatrix}0 \\ 0\end{bmatrix}, \begin{bmatrix}\sigma_\tau^2 & 0 \\ 0 & \sigma_\theta^2\end{bmatrix}\right). \tag{12}$$

where $\mathbf{x}^T(t) = \left[x_t^T, y_t^T, z_t^T\right]^\top$ is the target location, $\mathbf{v}^R(t)$ is the receiver's velocity vector, which depends on the vehicle's heading and pitch. $w^\tau(t)$ and $w^\theta(t)$ are the additive noise to the range and bearing, respectively.

The bistatic ambiguity problem results in the ambiguity function described in (10) which corresponds to points having the same bistatic range (i.e. belonging to the bistatic ellipsoid) and with bearing corresponding to the linear array conic ambiguity obtained from equation 9, with $R = tan\,(\theta)$.

Fig. 3 shows a conceptual representation of the uncertainty reduction that can be obtained with the proposed measurement model. When only one measurement (top row, left in Fig. 3) is available, the intersection between the bistatic ellipse and the ULA cone is not able to identify the depth of the target. However when more measurements are collected with different vehicle pitch angles, their intersection leads towards a reduction in the uncertainty of the target depth. The ability of the measurement model to identify the target in the $x-y$ plane is the same as that of the planar bistatic localisation case. Finally, measurement errors, missed detections and clutter are included as proposed in [17].

B. Estimation

The ULA measurements are non-linear function of the target state and can easily lead to non-trivial multi-hypothesis belief distributions [18], [19]. A convenient approach to incorporate such non-linear measurements and approximate the posterior of the target state is based on the use of particle filters [20], [21], [12]. Alternative approaches are of course possible, including those based on linearisation [17], [22]. One alternative and particularly appealing option in this case is based on using constrained satisfaction programming and interval analysis [23] since the problem can be approached in its full non linearity.

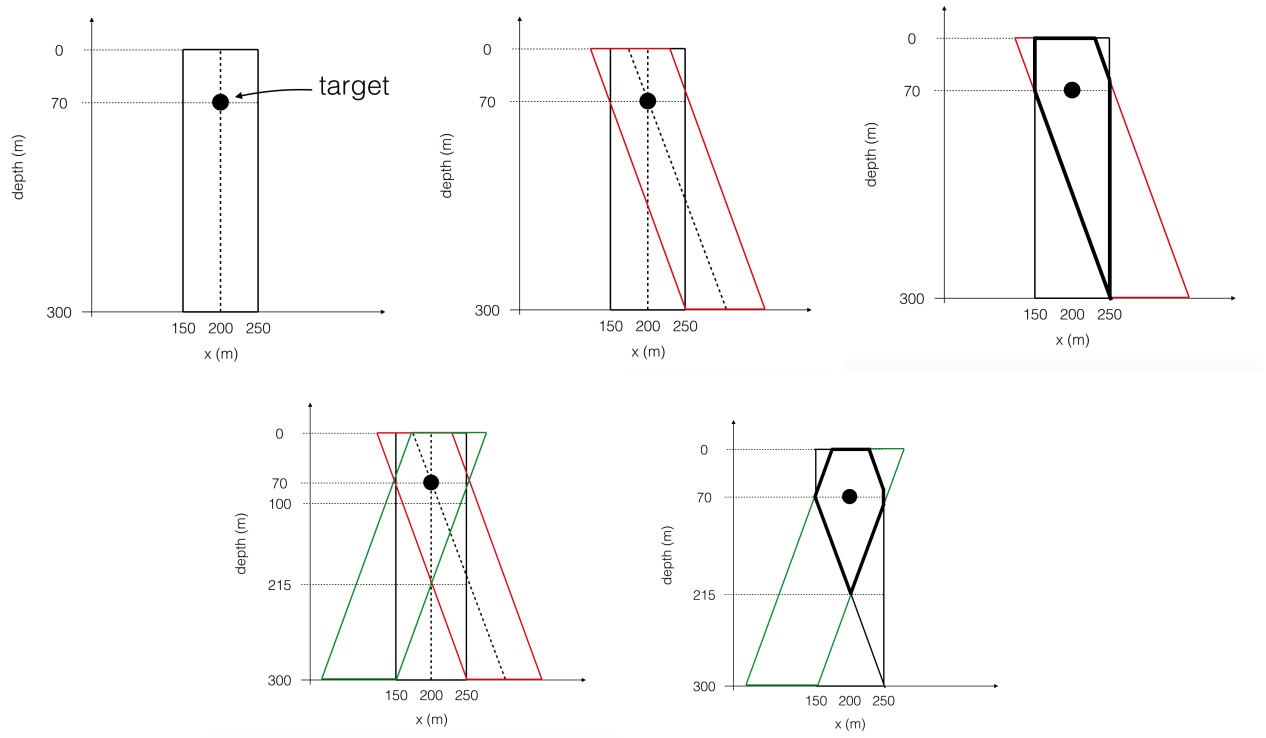

Fig. 3. Three dimensional localisation of a static target. Top row, left: Only one measurement is available and this leads to an uncertainty box where target depth cannot be discriminated. Top row, middle: the second available measurement is done with the AUV at a different pitch resulting in a tilted uncertainty box. Top row, right: the target position lies in the intersection of the measurement uncertainties leading to a reduced uncertainty in depth. Bottom row, left: a third measurement becomes available with yet another pitch angle. Bottom row, right: the target location belongs to the intersection of all three measurements hence further reducing the uncertainty in depth. Note that all depths below 215 m have been excluded.

In what follows we restrict our analysis to the Bayesian framework of particle filters. More formally, let $\mathbf{x}^T(t) = [x, y, z]^\top$ be the state of the target at time t, and $x_i^R(t)$ be the position of the i-th member of the team. We indicate with $S = \left[\mathbf{x}_1^R(t), \mathbf{x}_2^R(t), ..., \mathbf{x}_n^R(t)\right]$ the full configuration of vehicles, and we consider that at each ping each vehicle moves in the environment and makes up to K measurements $\mathbf{z}_i = \{z_{i,1}, z_{i,2}, ..., z_{i,K}\}$. The belief at time t is the distribution of state conditioned on all measurements up to time t, that are incorporated recursively in a typical Bayesian filter, and it is approximated as a weighted sum of Dirac delta functions in the particle filter approximation [24]:

$$bel(\mathbf{x}_t) = \eta p(\mathbf{z}_t|\mathbf{x}_t) \int bel(\mathbf{x}_{t-1}) p(\mathbf{x}_t|\mathbf{x}_{t-1}) d\mathbf{x}_{t-1} \approx \approx \sum_j \omega_j \delta(\mathbf{x}_t - \hat{\mathbf{x}}_j) \quad (13)$$

where η is a normalising constant, $\hat{x}_j$ is the position of particle j and ω_j is the associated weight. The target state estimate is finally calculated as the Minimum Mean Square Error (MMSE):

$$\mathbf{x}(t) = \int \mathbf{x(t)} P(\mathbf{x(t)}|Z_{1:t}) d\mathbf{x(t)} \approx \sum_j \omega_j \hat{\mathbf{x}}_j \quad (14)$$

C. Target motion model

The target is modeled through a nearly constant velocity model [17]:

$$\mathbf{x}(t) = A\mathbf{x}(t-1) + B\mathbf{v}(t) \quad (15)$$

where A is the state transition matrix, and B**v**(t) is used to include unmodeled dynamics. **v**(t) is assumed to be Gaussian distributed with zero-mean and covariance matrix $Q = \sigma_v^2 I$.

D. Vehicle control law

In order to exploit the advantages given by the 3D bistatic localisation, the vehicles need to move in the water column to obtain measurements that can reduce the uncertainty of the target estimate. In this paper, the vehicle follows the control law described in [13] to select their waypoint in the horizontal plane. According to this method, each vehicle calculates the full posterior of the target state; propagates the target state in the future according to target model and uses a performance prediction model (ARTEMIS [25]) that provides the detection probability as a function of target and receiver position to finally choose the path that will put the AUV in the best position to maximise the detection probability. The optimal path $\bar{u}$ is selected by each vehicle minimising the expected value of the probability of detection along a desired time horizon L:

$$\bar{u} = \arg max_{u_{k:k+L}} = \sum_{i=k+1}^{k+L} \left[\int P_D(\mathbf{x}, u) p(\mathbf{x}_i|\mathbf{z}) dx_i \right] \quad (16)$$

When more than one vehicle is present, the aggregative cost function proposed in [26] can be used.

Finally, the change in depth is chosen according to a pre-planned yo-yo pattern (see, for instance, Fig. 7, which shows the depth change of OEX Groucho during the REP16 trial). This solution has the advantage of maximising the usage of the span of the water column, minimising the number of pitch changes for the AUV. Since when the array bends too much the signal processing might not be able to correctly process the acoustic data, this approach has limits the number of turning required (up-down movements) by the vehicle and hence it limits the change in the array shape due to changes in depth.

IV. Simulations

This section reports simulation results to test the proposed scheme. We consider first the case in which the PD is uniform in the entire area. In this case, the ability of the proposed method to estimate the target's depth depends only on the spatial (or temporal) diversity that the system is able to obtain from the measurements. The first scenario considers two vehicles. The first vehicle (AUV1) starts at depth $0\,\mathrm{m}$ and moves towards its final depth of $50\,\mathrm{m}$ at a maximum pitch angle of $20°$, then it keeps constant depth. The second vehicle (AUV2) moves at a constant depth of $0\,\mathrm{m}$ throughout the mission. The target is moving at a constant depth of $50\,\mathrm{m}$, with a constant speed of $4\,\mathrm{m\,s^{-1}}$.

The initial condition of the scenario is shown in Fig. 4. Each vehicle is equipped with a uniform linear array to act as receiver of an active sonar with a pulse repetition rate (PRI) of $20\,\mathrm{s}$. Each AUV then shares its contacts with its teammate using a Time Division Multiple Access Protocol, with a $10\,\mathrm{s}$ repetition cycle. The probability of detection is uniform and set equal to $P_D = 0.7$. The particle filter is initialised with a uniform distribution in a box of $23\,\mathrm{km}$ x $30\,\mathrm{km}$ x $300\,\mathrm{m}$. The clutter is uniformly generated in the area of interest, whereas the target range and bearing measurements are considered to be affected by an additive noise with standard deviation: $\sigma_\tau = 0.0166$ s, $\sigma_\theta = 2.5$ deg.

The evolution of the particle filter target tracking on AUV2 is shown in Fig. 4 to Fig. 6 (a similar evolution is obtained for AUV1). Note how the filter is able to quickly discard all the depth solutions deeper than $150\,\mathrm{m}$ hence identifying it as a shallow target. After less then 10 pings, in this simulation, the MMSE then converges towards a depth of $75\,\mathrm{m}$ for both vehicles, which is within the uncertainty of the measurements. After 10 pings AUV1 has reached its maximum operating depth stabilising its attitude at $50\,\mathrm{m}$. From this moment on, there is no more spatial diversity in the measurements (both vehicles have $0°$ pitch) and the particles start to spread out again in the entire the water column.

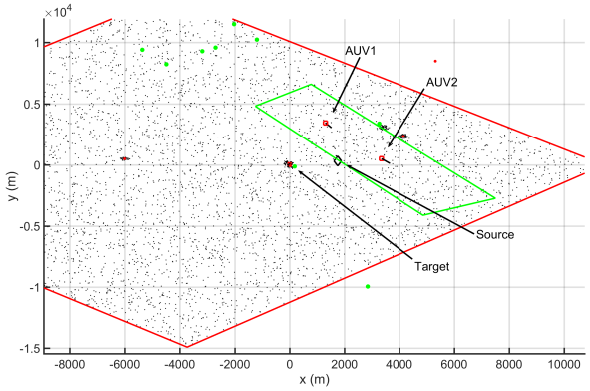

Fig. 4. Simulated scenario 1 after the first ping. The source is at depth $70\,\mathrm{m}$. The target moves at a constant depth of $50\,\mathrm{m}$. Particles are shown as black dots. Green dots are used to show AUV1's contact, red dots for those received from AUV2.

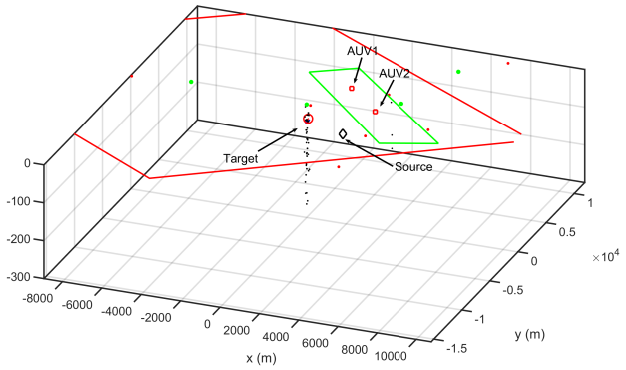

Fig. 5. Three dimensional view of the particle distribution on AUV2 after three pings. Note that most of the particles gathered in the first $100\,\mathrm{m}$ of the water column, identifying the target as shallow. In this specific case, the target depth MMSE was $40\,\mathrm{m}$.

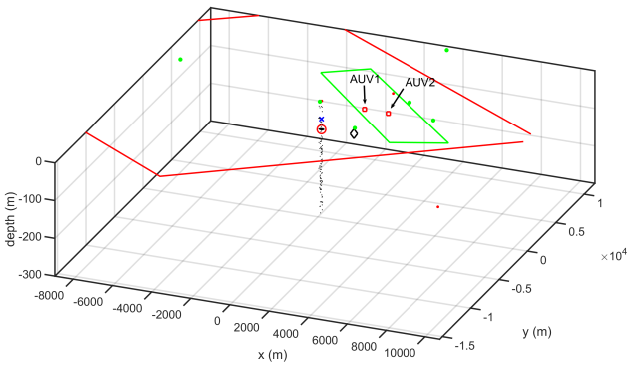

Fig. 6. Three dimensional view of the particle distribution on AUV2 after eight pings. Most of the particles are still in the first $100\,\mathrm{m}$ of the water column with a larger cluster at $75\,\mathrm{m}$. After this ping, AUV1 stabilised at $50\,\mathrm{m}$, with $0°$ pitch, hence not creating the necessary spatial diversity needed to localise the target depth and the particle quickly spread out along the water column.

V. Sea trial experimentations

A. REP16 Atlantic

The proposed approach was tested in real time during the Recognized Environmental Picture (REP) Atlantic 2016. The trial's objectives ranged from testing solutions for active and passive sonars, to AUV behaviours.

The deployed equipment included two moored gateway buoys, and two CMRE Ocean Explorer (OEX) AUVs. The two AUVs, OEX Groucho and OEX Harpo, are vehicles of 4.5 m length and a diameter of 0.53 m, which can operate at the maximum depth of 300 m. Their maximum speed is $1.5\,\mathrm{m\,s^{-1}}$ with a typical speed of $1\,\mathrm{m\,s^{-1}}$ while towing the linear array to have a battery endurance of about $16\,\mathrm{h}$.

Each OEX is equipped with a main computer and with a configurable payload section. The main computer directly commands the vehicle and maintains navigation. The payload section is used for on-board signal processing [14], and to run all the necessary communications components and for MOOS-IvP autonomous decision making, and it is where the algorithm presented has been implemented.

The vehicles are used in combination with the SLITA towed-arrays [27]. The array is composed of 83 hydrophones that can be used is sets of 32 to obtain the right sensor spacing for a desired operating frequency, which in this work is considered to be between $1\,\mathrm{kHz}$ and $4\,\mathrm{kHz}$.

The Deployable Experimental Multistatic Undersea Surveillance (DEMUS) source was used as primary active source for this experiment. DEMUS is a programmable bottom-tethered source capable of high source levels based on free-flooded ring technology. The source is connected to a radio buoy equipped with a GPS receiver which is used to have a very accurate position estimation during the trial and to synchronise the transmission times.

The target used for this experiment was an echo repeater moving at a constant speed and at a depth of $70\,\mathrm{m}$.

B. Results at sea

A preliminary test of the yo-yo based control law was performed during the initial phase of the trial. This made it possible to verify the ability of the vehicle to correctly followed the required depth change and to test the behaviour of the array during yo-yo movements so to understand the impact of having a tilted array during contact formation [14]. The vehicle depth change is shown in Fig. 7, with the real-time produced contacts reported in Fig. 8.

Except for this initial test however, for the rest of the experiment, we could not use the depth adaptation part of the behaviour and the vehicles were kept at a constant depth of $70\,\mathrm{m}$. For this reason, it was not possible to exploit the spatial and temporal diversity coming from depth changes. However, since the received signal SNR depends on the geometry of the bistatic system and of course on the specific environment encountered, including reverberation, bathymetry, sound speed, multipath time spreading, etc. the filter was still able to produce an estimation of the target depth relying on a non uniform P_D/signal to reverberation plus noise ratio (SRNR) calculated a priori using the ARTEMIS adiabatic normal mode model

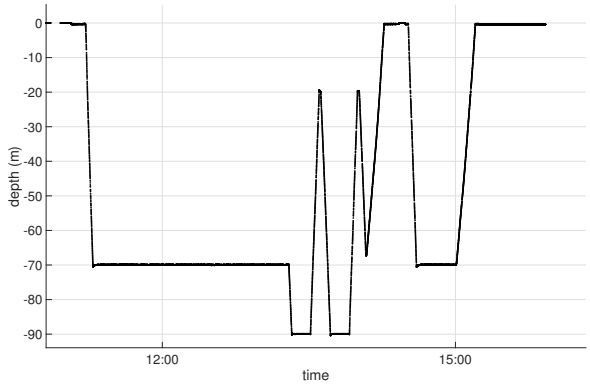

Fig. 7. Yo-yo movement followed by OEX Groucho during the REP16 sea trial to control its depth during the area search experiments.

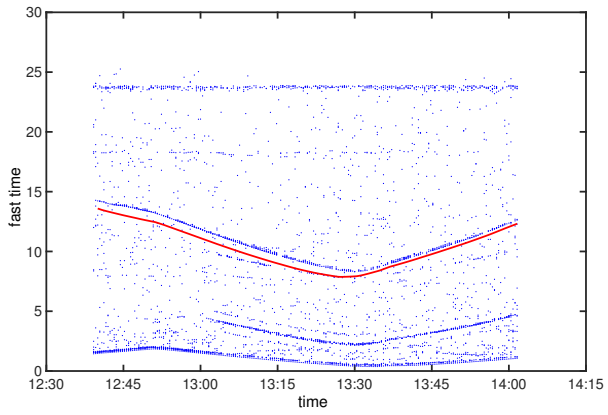

Fig. 8. Contacts produced by the real-time signal processing while OEX Groucho was performing the yo-yo pattern shown in Fig. 7.

[28], [29], [25] initialised with environmental parameters collected during the REP14 experiment that was held in 2014 in the same area. In this case, the target tracking filter, although not fully exploiting the three dimensional measurements, could still match its detection performance with its a-priori detection probability. Results are shown in Fig. 9. In the picture, the left column shows an x-y overview of the target tracking, while the right column shows the evolution of the particles with depth. The filter was initialised with a uniform distribution within a $15\,\mathrm{km}$x$15\,\mathrm{km}$ area (shown through the red box in Fig. 9) where the target was a-priori known to be. The filter was able to converge to the x-y target location within the first 50 pings, estimating the target depth to be $50\,\mathrm{m}$. At ping 85 a new hypothesis for the target depth was generated at $75\,\mathrm{m}$ hence reducing the error with respect to the correct depth of $70\,\mathrm{m}$. Unfortunately, short after this ping the real-time signal processing was not able to correctly detect the echo repeat target and we could not verify the convergence of the estimated depth towards the correct value.

VI. Conclusions

This paper proposed to tackle the target tracking problem in its full three dimensional aspects. Theoretical details have been given to generalise the bistatic localisation to a 3D

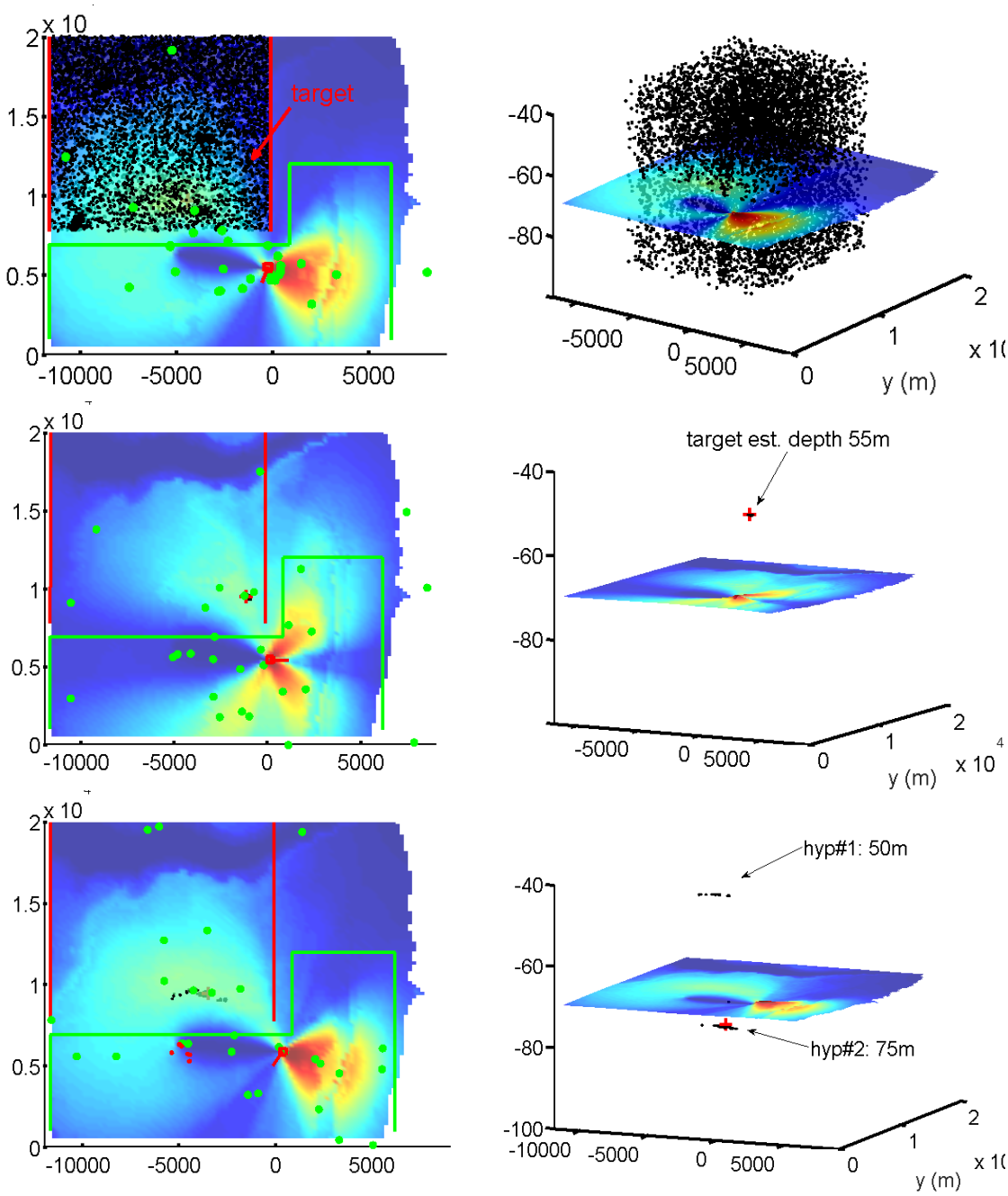

Fig. 9. Target tracking during the REP16 sea trial. The filter was initialised with a uniform distribution within a 15 kmx15 km area (shown through the red box in Fig. 9) where the target was a-priori known to be. The filter was able to converge to the x-y target location within the first 50 pings, estimating the target depth to be 50 m. At ping 85 a new hypothesis for the target depth was generated at 75 m hence apparently reducing the error with respect to the correct depth of 70 m. Unfortunately, short after this ping the real-time signal processing was not able to correctly detect the echo repeat target and we could not verify the convergence of the estimated depth towards the correct value.

scenario, and to include the cylindrical ambiguity of a linear array into the measurement model of a Bayesian filter. A method of navigation for AUVs has been presented. The approach is based on the Bayesian posterior produced by the available observations done by the network, and on a range-dependent acoustic model that is used to predict the target detection probability for a given source-receiver-target geometry. Coupling the full 3D measurement model with the predicted detection probability makes it possible to estimate the target depth together with its position in the $x - y$ plane. Results are shown through simulations and verified using data collected during the REP16 experimental campaign. Although these initial results are encouraging, more research is needed to better understand how the signal processing uncertainties might impact on the algorithm results.

ACKNOWLEDGMENT

The authors gratefully acknowledge all the NRV Alliance crew and the CMRE Engineering and Technological Department staff for their help, willingness and collaboration during the REP16 cruise. This work has been funded by NATO Allied Command Transformation.

REFERENCES

[1] A. Caiti, A. Munafo, and G. Vettori, "A Geographical Information System (GIS)-Based Simulation Tool to Assess Civilian Harbor Protection Levels," *IEEE Journal of Oceanic Engineering*, vol. 37, no. 1, pp. 85–102, 2012.

[2] S. Lemon, "Towed-array history, 1917-2003," *IEEE J. Ocean. Eng.*, vol. 29, no. 2, pp. 365–373, Apr. 2004.

[3] R. R. Kneipfer, "Sonar beamforming an overview of its history and status," NUWC-NL, Tech. Rep. AD-A250 189, May 1992.

[4] A. Caiti, V. Calabro, G. Dini, A. L. Duca, and A. Munafò, "Mobile underwater sensor networks for protection and security: field experience at the uan11 experiment," *Journal of Field Robotics*, vol. 30, no. 2, pp. 237–253, 2012.

[5] M. Hamilton, S. Kemna, and D. Hughes, "Antisubmarine warfare applications for autonomous underwater vehicles: The GLINT09 sea trial results," *J. Field Rob.*, vol. 27, no. 6, pp. 890–902, 2010.

[6] G.Ferri, A. Munafò, R. Goldhahn, and K. LePage, "A non-myopic, receding horizon control strategy for an auv to track an underwater target in a bistatic sonar scenario," in *in Proc. of CDC2014, Los Angeles*, 2014.

[7] I. F. Akyildiz, D. Pompili, and T. Melodia, "Underwater acoustic sensor networks: Research challenges," *Ad Hoc Networks (Elsevier)*, vol. 3, no. 3, pp. 257–279, Mar. 2005.

[8] A. Caiti, E. Crisostomi, and A. Munafo, "Physical Characterization of Acoustic Communication Channel Properties in Underwater Mobile Sensor Networks," Springer Berlin Heidelberg, Berlin, Heidelberg, 2010.

[9] M. Stojanovic and P.-P. J. Beaujean, "Acoustic communication," in *Handbook of Ocean Engineering*, M. R. Dhanak and N. I. Xiros, Eds. Springer, 2016.

[10] J. Alves, K. LePage, P. Guerrini, J. Potter, G. Zappa, T. Furfaro, A. Munaf, and A. Vermeij, "Underwater communications research and development at cmre," in *OCEANS 2015 - Genova*, May 2015, pp. 1–7.

[11] J. Potter, J. Alves, T. Furfaro, A. Vermeij, N. Jourden, D. Merani, G. Zappa, and A. Berni, "Software defined open architecture modem development at cmre. in underwater communications and networking," in *Proc. Intl. Conf. UComms*, 2014, pp. 1–4.

[12] P. Braca, P. Willett, K. LePage, S. Marano, and V. Matta, "Bayesian tracking in underwater wireless sensor networks with port-starboard ambiguity," *IEEE Trans. Signal Process.*, vol. 62, no. 7, pp. 1864–1878, 2014.

[13] R. Goldhahn, P. Braca, G. Ferri, A. Munafò, and K. LePage, "Adaptive bayesian bahaviours for auv surveillance networks," in *Conf. on Underwater Acoustics*, 2014.

[14] G. Canepa, A. Munafò, M. Micheli, S. Murphy, and L. Morlando, "Real-time continuous active sonar processing," in *IEEE/MTS Conf. OCEANS15*, 2015.

[15] R. Bajcsy, "Active perception," *Proceedings of the IEEE*, vol. 76, no. 8, pp. 996–1005, 1988.

[16] S. Coraluppi, "Multistatic sonar localization," *IEEE J. Ocean. Eng.*, vol. 31, no. 4, pp. 964–974, Oct. 2006.

[17] Y. Bar-Shalom, P. Willett, and X. Tian, *Tracking and Data Fusion: A Handbook of Algorithms*. Storrs, CT: YBS Publishing, Apr. 2011.

[18] S. Coraluppi and D. Grimmett, "Multistatic sonar tracking," in *Proc. of SPIE Conference on Signal Processing, Sensor Fusion, and Target Recognition XII*, Orlando FL, USA, Apr. 2003.

[19] M. Daun and F. Ehlers, "Tracking algorithms for multistatic sonar systems," *EURASIP Journal on Advances in Signal Processing*, pp. 1–28, 2010.

[20] M. S. Arulampalam, S. Maskell, N. Gordon, and T. Clapp, "A tutorial on particle filters for online nonlinear/non-Gaussian Bayesian tracking," *IEEE Signal Process. Mag.*, vol. 50, no. 2, pp. 174–188, Feb. 2002.

[21] O. Cappe, S. Godsill, and E. Moulines, "An overview of existing methods and recent advances in sequential Monte Carlo," *Proc. IEEE*, vol. 95, no. 5, pp. 899–924, 2007.

[22] S. J. Julier and J. K. Uhlmann, "Unscented filtering and nonlinear estimation," *IEEE Transactions on Signal Processing*, vol. 92, no. 3, pp. 401–422, Mar. 2004.

[23] J. Sliwka, A. Munafò, G. ferri, and J. Alves, "Interval methods based auv localization in the context of an acoustic network with experimental results."

[24] S. Thrun, D. Fox, and W. Burgard, *Probabilistic Robotics*. MIT press, 2005.

[25] C. Harrison, "Target time smearing with short transmissions and multipath propagation," *J. Acoust. Soc. Am.*, vol. 130, no. 3, pp. 1282–1286, 2011.

[26] R. Goldhahn, P. Braca, and K. LePage, "Adaptive bayesian behaviours for autonomous underwater vehicle surveillance networks," Centre for Maritime Research and Experimentation, Tech. Rep. CMRE-FR-2015-002, 2013.

[27] A. Maguer, R. Dymond, M. Mazzi, S. Biagini, and S. Fioravanti, "SLITA: a new slim towed array for AUV applications," in *Acoustics'08*, 2008, pp. 141–146.

[28] C. Harrison, "Fast bistatic signal-to-reverberation-ratio calculation," *Journal of Computational Acoustics*, vol. 13, no. 2, pp. 317–340, 2005.

[29] ——, "Closed-form expressions for ocean reverberation and signal excess with mode stripping and Lambert's law," *J. Acoust. Soc. Am.*, vol. 114, no. 5, pp. 2744–2756, 2003.

Document Data Sheet

Security Classification		Project No.
Document Serial No.	**Date of Issue**	**Total Pages**
CMRE-PR-2019-062	June 2019	8 pp.

Author(s)

Andrea Munafó, Gabriele Ferri, Kevin LePage, Ryan Goldhahn

Title

AUV active perception: Exploiting the water column

Abstract

Autonomous Underwater Vehicles (AUVs) present a low-cost alternative or supplement to existing underwater surveillance networks. The NATO STO Centre for Maritime Research and Experimentation is developing collaborative autonomous behaviours to improve the performance of multi-static networks of AUVs. In this work we lay the foundation to combine a range-dependent acoustic model with a three dimensional measurement model for a linear array within a Bayesian framework. The resulting algorithm is able to provide the vehicles with an estimation of the target depth together with the more usual information based on a planar assumption (i.e. target latitude and longitude). Results are shown through simulations and as obtained from the REP16 sea trial where for the first time a preliminary implementation of the method was deployed in the C-OEX vehicles.

Keywords

Receivers, time measurement, position measurement, uncertainty, sea measurements, sensor arrays

Issuing Organization

NATO Science and Technology Organization
Centre for Maritime Research and Experimentation

Viale San Bartolomeo 400, 19126 La Spezia, Italy

[From N. America:
STO CMRE
Unit 31318, Box 19, APO AE 09613-1318]

Tel: +39 0187 527 361
Fax:+39 0187 527 700

E-mail: library@cmre.nato.int